

Tetrabutylphosphonium-salicyl-imine-chitosan metallo-Schiff bases: Supramolecular architectures as multifunctional pharmacological materials.

Gelan A. Seif,^{a,*}Reda F. M. Elshaarawy,^bMehrez E. El-Naggar,^cTahia B. Mostafa,^{a,*}Emtithal A. El-Sawi^a

^aDepartment of Chemistry, Faculty of Women for Arts, Science and Education, Ain Shams University, Heliopolis, Cairo, Egypt

^bDepartment of Chemistry, Faculty of Science, Suez University, Suez, Egypt.

^cPre-Treatment and Finishing of Cellulosic Fabric Department, Textile Research Division, National Research Center, Cairo, Egypt

Abstract

The current work provides a simple synthetic route for the preparation of poly-(phosphonium-salicyl)-grafted chitosan Schiff bases (PPCSB), its M(II) complexes (M = Cu or Pd) and silver nanobiocomposites (NBCs). The *ex-situ* protocol was used for preparation of nanosilver (AgNPs) using NaBH₄ as a reducing agent then capped either by PPCSB or Pd(II)PPCSB to fabricate NBCs {AgNPs@PPCSB, AgNPs@Pd(II)PPCSB}. Structural, morphological and physicochemical characterizations of the new architectures were examined based upon diverse spectral and microscopic techniques. The antibacterial properties of new compounds were investigated against gram positive (*S. aureus*, *B. subtilis*) and gram negative (*E. coli*, *P. aeruginosa*) bacterial strains. Unexpectedly, the M(II)PPCSB complexes were found to be more active against all tested bacterial strains than NBCs (AgNPs@PPCSB, AgNPs@Pd(II)PPCSB). Meanwhile, as revealed from ZOI values, the Cu(II)PPCSB is the most potent bactericidal agent against all tested bacterial strains except *E. coli* species which is more affected by Pd(II)PPCSB

Keywords: tributylphosphonium, *ex-situ* AgNPs, Cu(II)/ Pd(II) complexes, Nanobiocomposites, antimicrobial activity.

1- Introduction

Chitosan (CS) is one of the most readily available biopolymer due to preparing it from alkaline N-deacetylation of Chitin, which is the most plentiful polysaccharide in nature. The structure of chitosan is a linear co-biopolymer of 2-acetamido-2-deoxy-β-D-glucopyranose (GluNHAc) with 2-amino-2-deoxy-β-D-glycopyranose (GluNH₂) (Rinaudo, M., 2006). Due to the unique properties of chitosan such as a biocompatibility, biodegradability and also its antimicrobial and anti-cancer activity (Choi et al., 2001, Chung et al., 2012, Foster et al., 2015, Xia et al., 2011), CS is very attractive for many applications in the pharmaceutical, agricultural, food, textiles and medical fields and cosmetic industries and a treatment for waste water (Crini, G., 2006, Khor et al., 2003, Miretzky et al., 2009). Moreover, many studies have shown that the modification of chitosan via Schiff bases condensation between primary amines and aldehydes increases its biological activity.

***Corresponding authors:** GAS, E-mail: saragain20@yahoo.com
TBM, E-mail: tahia_mostafa@yahoo.com

That is due to appearance of azomethine bond ($-C=N$) (Verlee et al., 2017, Elshaarawy et al., 2016, Raman et al., 2011, Salama et al., 2015).

In addition to promote antimicrobial and antitumor action of CS Schiff bases by introducing metal ions as a complexes such as Cu(II) and Pd(II) (Abdelwahab et al., 2015, Antony et al., 2013, Baran, 2017, Garoufis et al., 2009, Han et al., 2014) or metal nanoparticles as Ag-NPs composites (Wang et al., 2011). Therefore, to improve the biological activity of chitosan in our present study, new polyphosphonium-based macromolecular chitosan Schiff base ligand (PPCSB) will be synthesized from the reaction between CS with tributylphosphonium-based 3-ethyl-salicylaldehyde. Then, this macromolecular Schiff base will be used as either a chelating ligand for Cu(II)/ Pd(II) ions to prepare the corresponding M(II) complexes ($M = Cu$ or Pd), or, as a capping agent for silver nanoparticles (AgNPs) to form new AgNPs-nanobiocomposite (AgNBC).

2- Materials and methods

Mining of shrimp shells into chitin followed by its partial deacetylation to prepare CS and, eventually, partial oxidation degradation of CS was the protocol used to fabricate oligochitosan (OC) as described in our earlier work (Elshaarawy et al., 2019).

2.1. Materials

Chemicals were obtained from the following suppliers and used without further purification: 2-ethylphenol, anhydrous $MgCl_2$, tri- n -butylphosphine (nBu_3P) (Sigma–Aldrich), paraformaldehyde ($(CH_2O)_n$) (Roth), triethyl amine (Et_3N) and anhydrous zinc chloride ($ZnCl_2$) (Grüssing GmbH), silver (I) nitrate ($AgNO_3$), copper(II) acetate monohydrate ($Cu(CH_3COO)_2 \cdot H_2O$) and palladium(II) chloride $PdCl_2$ (Acros).

2.2. Instrumentation

Elemental analyses for C, H, N and S were performed with a Perkin–Elmer 263 elemental analyzer. FT-IR spectra were recorded on a BRUKER Tensor-37 FT-IR spectrophotometer in the range $400–4000\text{ cm}^{-1}$ as KBr discs or in the $4000–550\text{ cm}^{-1}$ region with 2 cm^{-1} resolution with an ATR (attenuated total reflection) unit (Platinum ATR-QL, Diamond). For signal intensities the following abbreviations were used: br (broad), sh (sharp), w (weak), m (medium), s (strong), vs (very strong). NMR-spectra were obtained with a Bruker Avance DRX200 (200 MHz for 1H) or Bruker Avance DRX500 (500 MHz for ^{13}C) spectrometer with calibration to the residual proton solvent signal in DMSO- d_6 (1H NMR: 2.52 ppm, ^{13}C NMR: 39.5 ppm), $CDCl_3$ (1H NMR: 7.26 ppm, ^{13}C NMR: 77.16 ppm) against TMS with $\delta = 0.00$ ppm. Multiplicities of the signals were specified s (singlet), d (doublet), t (triplet), q (quartet) or m (multiplet). The electrospray ionization mass spectra (ESI-MS) of the synthesized compounds were acquired in the linear mode for positive ions on UHR-QTOF maXis 4G (Bruker Daltonics) and Bruker Ultraflex MALDI-TOF instrument equipped with a 337 nm nitrogen laser pulsing at a repetition rate of 10 Hz. The 2+ charge assignment of ions in ESI-MS was confirmed by the $m/z = 0.5$ difference between the isotope peaks (x , $x+1$, $x+2$). Peaks with chlorine showed the isotope ratio $^{35/37}Cl = 75.8:24.2$. For the mass spectral assignment: Peaks are based on ^{12}C with 12.0000 Da and ^{35}Cl with 34.968 Da. The morphology of the new compounds was investigated by using Scanning electron microscopy

(SEM Hitachi S-7400, Hitachi, Japan). The elemental analysis of the formed products was determined by utilizing energy dispersive –X-ray (EDX) connected to SEM instrument.

2.3. Synthesis of 3-ethylsalicylaldehyde (1)

To a stirred mixture of dry anhydrous magnesium dichloride (9.52 g, 100 mmol) and dry paraformaldehyde (4.50 g, 150 mmol) in dry Acetonitrile (ACN) (200 ml) was added drytriethylamine(26.1 ml, 185 mmol) dropwise and the mixture was stirred at room temperature for 15 min under nitrogen atmosphere. 2-Ethylphenol (6.20 g, 50.0 mmol) was then added dropwise, resulting an opaque, light pink mixture. This solution was heated at gentle reflux temperature under nitrogen for ca. 3 h, during which time the color of the reaction mixture changes from light pink to orange. The solution was allowed to cool to room temperature then 200 mL of 1 N HCl was added followed by stirring for 30 min. The product was extracted with diethyl ether (5 x/75 ml portions) and the ether fractions collected together and washed with 1 N HCl (2 x 100 mL) and saturated NaCl_{aq} (3 x/100 ml portions). The ether layer was dried over anhydrous MgSO₄ followed by filtration. Volatiles were removed under reduced pressure to yield the corresponding salicylaldehyde, usually contaminated with the starting phenol. The crude product which was purified by column chromatography on silica gel using petroleum ether/ethyl acetate (90:10) mixture as the eluent to give pure 3-ethylsalicylaldehyde (68%) as a pale yellow oil. ¹H NMR (200 MHz, CDCl₃) δ (ppm): 11.45 (s, 1 H), 10.38 (s, 1 H), 7.58 (d, *J* = 7.4 Hz, 1 H), 7.47 (d, *J* = 7.3 Hz, 1 H), 7.11 (dd, *J*₂ = 7.6 Hz, *J*₁ = 1.8 Hz, 1 H), 2.81 (q, *J* = 7.8 Hz, 2 H), 1.30 (d, *J* = 7.7 Hz, 3H). ¹³C NMR (125 MHz, CDCl₃) δ (ppm): 192.11, 161.09, 137.79, 134.68, 130.14, 128.33, 122.21, 23.15, 15.08.

2.4. Synthesis of 5-chloromethyl-3-ethylsalicylaldehyde (2)

These compounds were synthesized from the corresponding salicylaldehydes according to the modified chloromethylation procedure (Elshaarawy *et al.*, 2014). In a typical synthesis, (2.28, 15.2 mmol) of 3-ethylsalicylaldehyde were treated with para-formaldehyde (1.0 g, 33.3 mmol) and zinc chloride (0.2 g, 1.46 mmol) in 11 ml of concentrated hydrochloric acid. The mixture was vigorously stirred under HCl_g atmosphere for 24-72 h at 313 K. The reaction mixture was extracted several times with diethyl ether (3x15 mL). Then the collected ether fractions were washed by 2x10 mL 5% aqueous NaHCO₃ solution, 2x10 mL brine, 5x10 mL milli-Q water and dried over anhydrous MgSO₄. After filtration and removal of the volatiles under reduced pressure, the obtained product was characterized and used in the next step without further purification. It is obtained as faint yellow crystals (92%). FTIR (KBr, cm⁻¹): 3510 (m, br), 3089 (m, br), 2971 (m, sh), 1647 (vs, sh), 1446, 1385 (s, sh), 1274 (s, sh), 690 (s, sh). ¹H NMR (200 MHz, CDCl₃) δ (ppm): 11.47 (s, 1 H), 10.42 (s, 1 H), 7.51 (s, 1 H), 7.48 (s, 1 H), 4.68 (s, 2 H), 2.72 (q, *J* = 8.0 Hz, 2 H), 1.28 (d, *J* = 7.9 Hz, 3H). ¹³C NMR (125 MHz, CDCl₃) δ (ppm): 192.31, 161.16, 138.05, 137.12, 131.29, 129.63, 128.87, 46.75, 24.06, and 15.18.

2.5. Synthesis of tributyl(3-ethyl-5-formyl-4-hydroxybenzyl)phosphonium chloride

To a vigorously stirred solution of ⁿBu₃P(2.25 g, 23.39 mmol) in dry toluene (10 mL) at room temperature was added the solution of 5-chloromethyl-3-ethylsalicylaldehyde (2)(4.15 g, 19.50 mmol) in dry toluene (10 mL), drop-wise over 30 min, under nitrogen atmosphere.

The resulting solution was stirred under nitrogen atmosphere at 60 °C for 24 h. After cooling, the isolated products were washed intensively with 2 x 5 mL dry toluene, several with ether (5x10 mL), to remove the unreacted materials, and dried under vacuum to give the desired products which used for the following preparations without further purification. It was isolated as a yellowish-white solid, (89%); mp 62-63 °C. FT-IR (KBr, cm^{-1}): 3433 (m, br), 3049 (m, sh), 2956 (m, sh), 1653 (vs, sh), 1532, 1458, 1398 (s, sh), 1276 (s, sh), 771 (vs, sh). ^1H NMR (200 MHz, CDCl_3) δ (ppm): 10.69 (s, 1 H), 10.18 (s, 1 H), 7.52 (d, $J = 2.00$ Hz, 1 H), 7.46 (s, br, 2 H), 4.63 (s, 2 H), 2.85 (t, $J = 7.1$ Hz, 6H), 2.68 (q, $J = 7.2$ Hz, 2H), 1.58-1.57 (m₍₅₎, 6H), 1.41-1.28 (m₍₆₎, 6H), 1.25 (t, $J = 7.2$ Hz, 3 H), 1.01 (t, $J = 6.8$ Hz, 9H). ^{13}C NMR (125 MHz, CDCl_3) δ (ppm): 192.48, 158.11, 138.89, 137.03, 130.32, 129.21, 127.97, 32.02, 26.55, 26.49, 22.79, 18.82, 15.10 and 13.99. ESI MS: In positive mode peaks at m/z 365.4 a.m.u. ($[\text{C}_{22}\text{H}_{38}\text{O}_2\text{P}]^+$, $[\text{M} - \text{Cl}]^+$)

2.6. Synthesis of polyphosphonium-based chitosan Schiff base (PPCSB) ligand

1 g of OC was dissolved in 100 mL of mixed solvent system of (2% AcOH_{aq} /EtOH, 1:1 V/V) by stirring at room temperature for 30 min, then, a solution of tetrabutylphosphonium-ethylsalicylaldehyde ionic liquid (Equimolar to the amino content of OC) in EtOH (30 mL) was added to the OC solution over 30 min at 70 °C with vigorous stirring. The reaction mixture was stirred for an additional 24 h at the same temperature and concentrated under reduced pressure to yield a jelly product which was diluted with an excessive amount of AcOEt and solidified using ultrasonic irradiation for 3 h. The isolated solid was filtered off and washed with EtOH/ AcOEt mixtures (30:70, 20:80, and 0:100 V/V, respectively). Finally, the PPCSB was dried at 35 °C under vacuum for 24 h. It was obtained as a yellow powder, Yield (1.69 g). FTIR (KBr, cm^{-1}): 3430 (vs, br), 3065 (m, sh), 2921 (m, br), 1637 (m, sh), 1511 (m, sh), 1464 (m, sh), 1376 (m, sh), 1287 (m, sh), 1155 (m, sh), 1096 (s, sh), 830 (w, sh), 717 (m, sh), 626 (m, sh), 561 (m, sh). ^1H NMR (600 MHz, 1% $\text{CD}_3\text{COOD}/\text{D}_2\text{O}$)_{60 °C} δ (ppm): 10.35 (s, 2H, Ar-OH), 8.22 (s, 2H), 8.22 (s, 1H), 7.46 (s, 2H), 7.19 (s, 2H), 5.71-5.58 (m, 4H), 5.23 (s, br, 2H), 4.65 (s, 4 H), 4.31-4.19 (m, 4H), 4.15-4.04 (m, 4H), 4.01-3.87 (m, 4H), 3.83-3.70 (m, 4H), 3.67 (t, $J = 7.1$ Hz, 4H), 3.64 (s, 4H), 3.59 (s, 4H), 3.44-3.22 (m, 8H), 2.74 (q, $J = 7.2$ Hz, 4H), 2.51 (t, $J = 7.0$ Hz, 12 H), 1.43-1.28 (m, 12H), 1.25 (t, $J = 7.2$ Hz, 6H), 1.22-1.09 (m, 12H), 0.99 (t, $J = 6.8$ Hz, 18H). ^{13}C NMR (151 MHz, 1% $\text{CD}_3\text{COOD}/\text{D}_2\text{O}$)_{60 °C} δ (ppm): 175.51, 161.33, 158.02, 138.12, 134.23, 129.07, 128.96, 127.52, 127.43, 125.28, 125.06, 110.34, 109.31, 86.19, 83.43, 80.62, 80.58, 79.74, 78.13, 75.87, 71.41, 71.19, 69.23, 68.84, 66.19, 63.28, 53.21, 34.76, 31.98, 26.52, 22.78, 19.02, 14.99 and 14.03. Anal. Calcd. for $\text{C}_{71}\text{H}_{120}\text{Cl}_2\text{N}_4\text{O}_{19}\text{P}_{22}$ (monomeric unit of PPCSB) (M = 1466.58): C, 58.15; H, 8.25; N, 3.82; Found: C, 57.99; H, 8.36; N, 3.79.

2.7. Preparation of Cu(II)-PPCSB complex

Initially, the PPCSB ligand (0.3 g) was dissolved in 1% AcOH_{aq} (30 mL) by stirring 70 °C to give a clear light yellow solution. Then, an aqueous solution of $\text{Cu}(\text{CH}_3\text{COO})_2 \cdot \text{H}_2\text{O}$ (0.3 g/ 10 mL H_2O) was added to this solution under continuous stirring at 70 °C for 8 h. At the end of the reaction time, the solution was cooled to room temperature and the isolated dark green precipitate was filtered out, washed several times with distilled water and dried under vacuum at 50 °C for 12 h. Yield (48%). FTIR (KBr, cm^{-1}): 3415 (vs, br), 2944 (m, br), 1730

(m, sh), 1648 (m, sh), 1558 (m, sh), 1378 (m, sh), 1247 (m, sh), 1155 (m, sh), 1070 (s, sh), 898 (m, sh), 767 (m, sh), 629 (m, sh), 566 (m, sh), 471 (m, sh).

2.8. Preparation of Pd(II)-PPCSB complex

Initially, the PdCl₂ aqueous solution was prepared by dissolving PdCl₂ (0.3 g) and HCl (0.5 g) in 10 mL water under stirring for 1 h at room temperature to obtain a clear aqueous solution of pH 2.1. Then, the PdCl₂ solution was gradually added to a suspension of PPCSB (0.3 g) in methanol (15 mL) and the reaction mixture was stirred at refluxing temperature for 9 h. Thereafter, the solution was cooled, and the formed precipitate was filtered out, washed with methanol and dried under vacuum at 50 °C. Pd(II)-PPCSB was obtained as a dark brown powder, Yield (55%). FTIR (KBr, cm⁻¹): 3442 (s, br), 2925 (m, sh), 1630 (m, sh), 1513 (m, sh), 1384 (m, sh), 1246 (m, sh), 1155 (m, sh), 1067 (s, sh), 762 (m, sh), 564 (m, sh), 423 (m, sh), 410 (vs, sh).

2.9. Preparation of AgNPs-based NBCs

At first, AgNPs were prepared as follow; a solution of AgNO₃ (0.3 g/10 mL H₂O) was added drop-wise to an aqueous solution of sodium borohydride (2.9 M, 6.6 mL) containing 1 mL of NaOH (0.001 M) and kept under stirring at 70 °C for 60 min. The color of colloidal solution was turned to yellow color upon the addition of AgNO₃. At the end of 60 min, the resulted solution of AgNPs was added to the suspended solution of PPCSB/Pd(II)-PPCSB (0.3 g) in 40 wt.% toluene and stirred at 80 °C for 6h. At the end of reaction, the solids of PIVCSBs loaded with the *ex-situ* AgNPs were collected by centrifugations. Afterwards, the precipitate was washed at least seven times with water-acetone (81/19, w/w) and then dried in air. The resultant powders were nominated as AgNPs@PPCSB/AgNPs@Pd(II)-PPCSB NBCs.

AgNPs@PPCSB was obtained as a brown powder, Yield (43%). FTIR (KBr, cm⁻¹): 3412 (s, br), 2919 (s, br), 1633 (s, sh), 1548 (m, sh), 1462 (m, sh), 1377 (m, sh), 1247 (m, sh), 1155 (m, sh), 1071 (vs, sh), 833 (w, sh), 615 (m, sh), 564 (m, sh), 421 (m, sh).

AgNPs@Pd(II)-PPCSB was obtained as a reddish brown powder, Yield (39%). FTIR (KBr, cm⁻¹): 3430 (vs, br), 2922 (m, sh), 1632 (s, sh), 1384 (s, sh), 1253 (m, sh), 1073 (vs, sh), 896 (m, sh), 614 (m, sh), 576 (m, sh), 468 (m, sh).

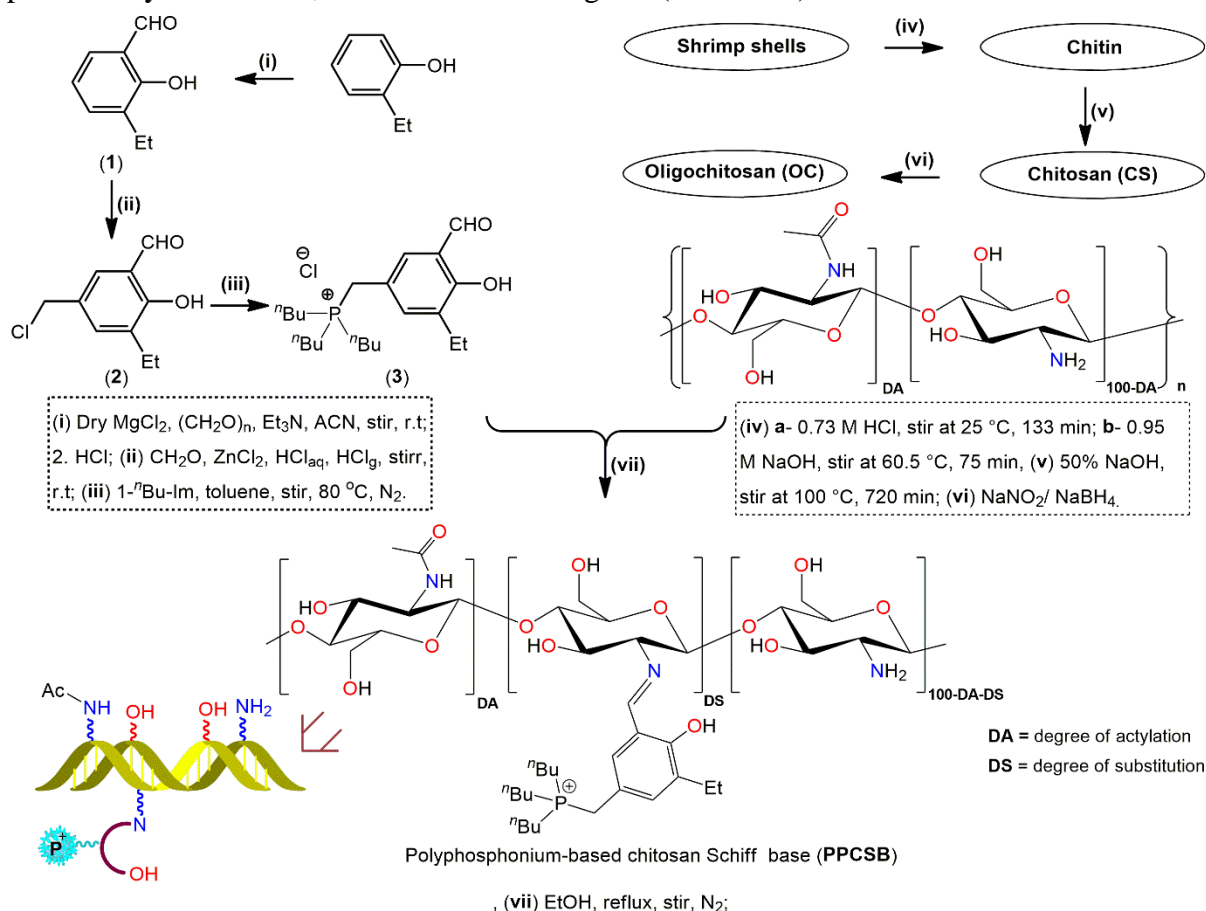
2.10. Antimicrobial Test

Disc agar plate method was employed to evaluate the antimicrobial activity of the as prepared compounds against many species of hazardous bacteria. The antimicrobial activities of the synthesized samples were placed on agar plates seeded with test microbes and incubated for 24h at the appropriate temperature of each test organism. Samples were tested against four different microbial strains *Staphylococcus aureus* (*S. aureus*) and *Bacillus subtilis* (*B. subtilis*) (as Gram⁺ bacteria) as well as *Pseudomonas aeruginosa* (*P. aeruginosa*) and *Escherichia coli* (*E. coli*) (as Gram⁻ bacteria). The bacterial test microbes were grown on a nutrient agar medium (DSMZ1) of the following components (g/L): Peptone (5.0), meat extract (3.0), agar (20.0), distilled water (1000.0 ml) and the pH to 7.0. The culture of each test microbe was diluted by distilled water (sterilized) to about 10⁷ - 10⁸ cells/ml, then 1ml of each was used to inoculate 1L-Erlenmeyer flask containing 250mL of solidified agar media then poured in Petri

dishes (10cm diameter containing 25ml). Films (5 mm diameter) were placed on the surface of the agar plates previously inoculated with the test microbe and incubated for 24 h at 37 °C. The tested microorganisms were obtained from the culture collection center, Microbial Chemistry Department, National Research Center, Egypt.

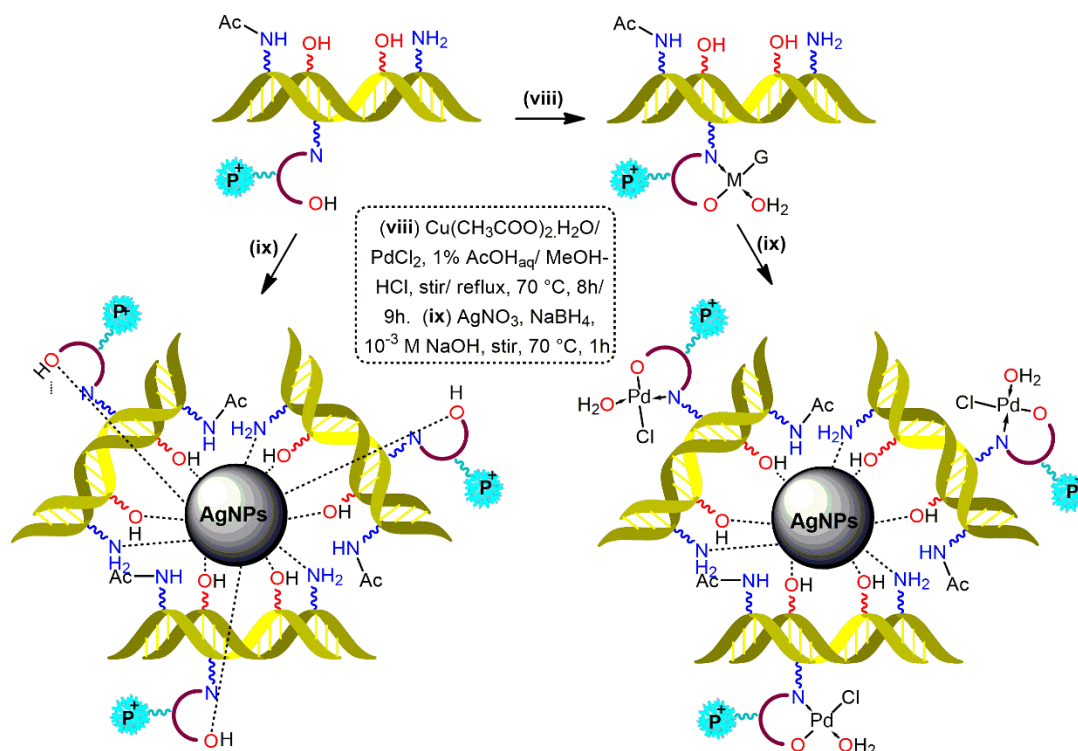
3- Results and Discussion

Multiple strategies have been used to synthesize PPCSB, its complexes and AgNPs- based NBCs, as well. Foremost, tributylphosphonium-ethylsalicylaldehydechloride (TBPESC, **3**) was synthesized starting from 3-ethylsalicylaldehydethrough consecutive chemical reactions (formylation, chloromethylation and quarternization) following a reported protocol (Elshaarawy *et al.*, 2014) with a slight modification. Then, the tributylphosphonium-ethylsalicylaldehyde salt (**3**) was grafted on the surface OC via a Schiff base condensation process to yield PPCSB, a macromolecular ligands (Scheme 1).



Scheme 1: Diagrammatic pathway for preparation of tributylphosphonium-ethylsalicylaldehydechloride (**3**), OC, and PPCSB.

Meanwhile, PPCSB was used as a chelating ligands in coordination to M(II) ions ($\text{M} = \text{Cu}$, Pd) through the N-(salicylidene) fragment distributed on the surface of PPCSB, by the reaction of PPCSB with $\text{Cu}(\text{CH}_3\text{COO})_2 \cdot \text{H}_2\text{O}$ and PdCl_2 to yield M(II)PPCSB complexes. On the other hand, AgNPs-based NBCs ($\text{AgNPs}@PPCSB/\text{AgNPs}@Pd(II)\text{-PPCSB}$ NBCs) were fabricated as follow; the AgNPs were initially prepared separately by reduction of AgNO_3 with NaBH_4 , thereafter, the AgNPs were loaded from the NPs dispersion onto the PPCSB/ Pd(II)PPCSB networks to offer the desired NBCs (Scheme 2).



Scheme 2: Preparation of M(II)PPCSB complexes (M, G = Cu, CH₃COO; Pd, Cl), AgNPs-based NBCs {AgNPs@PPCSB, AgNPs@Pd(II)PPCSB}.

3.1. Structural characterization

The degree of acetylation (DA) for OC and degree of substitution (DS) of PPCSB were calculated based on their elemental analysis according to our earlier work (Elshaarawy et al., 2016) and were found to be 26.13 and 44.93, respectively.

The successful grafting of salicyl-tributylphosphonium chloride on the surface of OC could be proved from different spectral techniques. Preliminarily, the emergence of two new stretches in the FTIR spectrum of PPCSB (Fig. 1) at 1633 and 1287 cm⁻¹, invisible in OC spectrum, characteristic for azomethinic (H-C=N) and phenolic (Ar-O) groups, offers the first supporting evidence for the successful grafting. Meanwhile, growth of new absorption bands at 1464, 1096, and 717 cm⁻¹ distinctive for ⁿBu₃(Cl)P⁺- fragment is indicative of the spreading of tributylphosphonium chloride motifs on the surface of OC. The steadfastness of the amino group of OC in preserving its involvement in the FTIR spectrum of PPCSB confirms the partial Schiff base condensation between the glucosamine (GlcNH₂) units and tributylphosphonium-salicylaldehyde chloride. This is consistent with the elemental analysis data which was used to estimate the degree of Schiff base condensation (degree of substitution, DS) in the aforementioned part. Moreover, FTIR spectral results offer initial proof for the success of chelation of PPCSB with M(II) ions (M = Cu, Pd) to form M(II)PPCSB and capping of AgNPs by PPCSB in preparation of AgNPs-based NBCs. Moreover, it gives insight into the potential functional groups of PPCSB involved in these processes. Where the fluctuation in the intensity and/ or the position of native FTIR stretches along with emergence of new absorption bands in the spectra of M(II)PPCSB complexes and NBCs confirms their successful fabrication (Fig. 1). Furthermore, the energy-shift in the absorption bands distinctive for the azomethinic (H-C=N) and phenolic (Ar-O)

stretches in the spectra of complexes and NBCs ($\Delta\nu_{C=N} = (-5)$ to $(+11)\text{cm}^{-1}$; $\Delta\nu_{Ar-O} = \sim (-40)\text{cm}^{-1}$) as compared with the spectrum of PPCSB confirms the participation of azomethinic N-atom and phenolate O-atom in complexation to M(II) ions and enveloping of AgNPs.

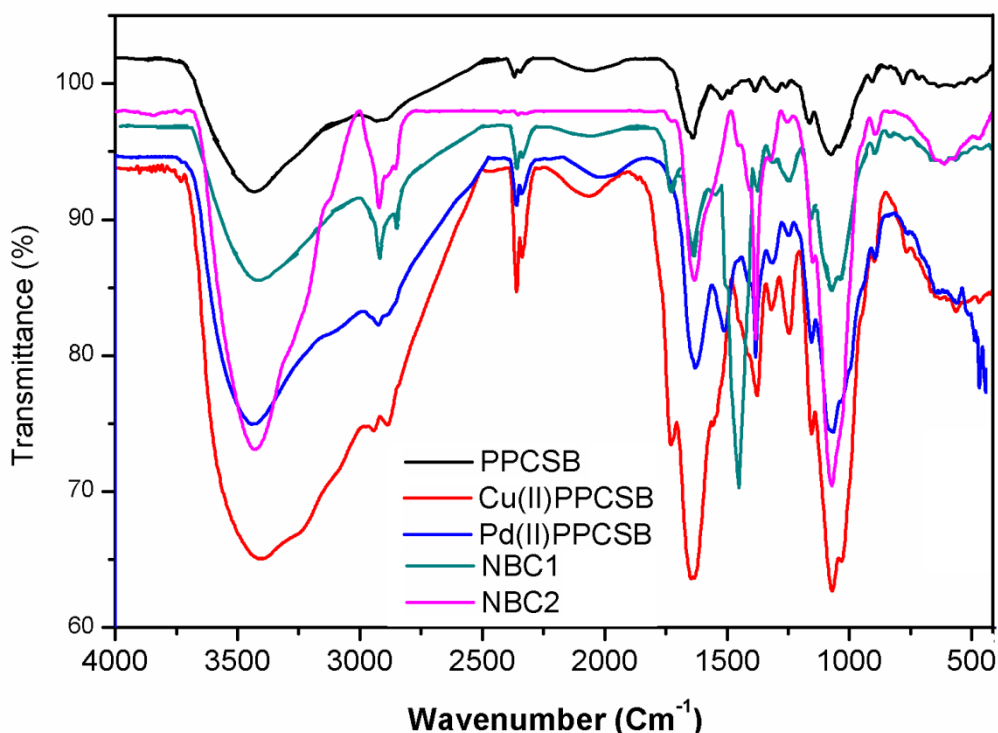


Fig. 1: The vibration pattern for the ATR-FTIR spectra of PPCSB, M(II)PPCSB complexes (M = Cu, Pd), NBC1 (AgNPs@PPCSB) and NBC2 (AgNPs@Pd(II)PPCSB).

Notable the emergence of a new intense shoulder into the Cu(II)PPCSB spectrum at 1730cm^{-1} , distinctive of acetate group, proving the participation of acetate anion in chelation of Cu(II) ion. The significant broadening of OH signature in the spectra of NBCs is indicative of sharing alcoholic OH groups of OC backbone in capping of AgNPs. Moreover, notice of a new intense peak in the IR spectra of NBCs at $1451 \pm 1\text{cm}^{-1}$, distinctive for AgNPs, confirm the successful loading of AgNPs on PPCSB and Pd(II)PPCSB.

The $^1\text{H-NMR}$ spectrum of PPCSB is consistent with the successful grafting of TBPECS on the surface OC with poly(ionic liquid) brushes as revealed from the observation of highly de-shielded singlets at a low-field region ($\delta = 10.26$ and 8.72ppm) attributable for the resonance of phenolic and azomethinic protons, respectively, engaged in an intramolecularly H-bonded environment. Moreover, the observation of sets of signals at the lower-field area $^1\text{H-NMR}$ spectrum ($8.72\text{--}7.55\text{ppm}$) assignable to aromatic protons. Meanwhile, $^{13}\text{C-NMR}$ spectrum of PPCSB offer further evidence for its successful fabrication as inspired from observation of two sets of $^{13}\text{C-NMR}$ peaks; (i) A lower field $^{13}\text{C-NMR}$ signals set (176 , ~ 162 , ~ 153 and $152\text{--}118\text{ppm}$) characteristic for the carbonyl, azomethinic, phenolic carbons and carbon skeleton of imidazolium-vanillylidene segments, respectively. (ii) A medium to higher field $^{13}\text{C-NMR}$ peaks in the range of $112\text{--}27\text{ppm}$ ascribed to the resonances of carbon backbone belong to the biopolymer chain confirming retention of the structural identity for

this biopolymer even after its surface functionalization.

3.2. Morphological characterization

The surface structure of the as prepared parent ligand, its M(II)PPCSB complexes (M = Cu, Pd), NBC1 (AgNPs@PPCSB) and NBC2(AgNPs@Pd(II)PPCSB) was investigated using SEM technique (Fig.2). It is clearly seen that the surface of PPCSB exhibited a rod-like particles. Whilst, small particles are developed of its surface upon the addition of the *ex-situ* synthesized AgNPs due to the deposition of these nanoparticles as shown in Fig.2 (D and E). Nevertheless, these particles have different shapes and size due to the absence of stabilizing agent during the preparation of AgNPs using NaBH₄ as a reducing agent.

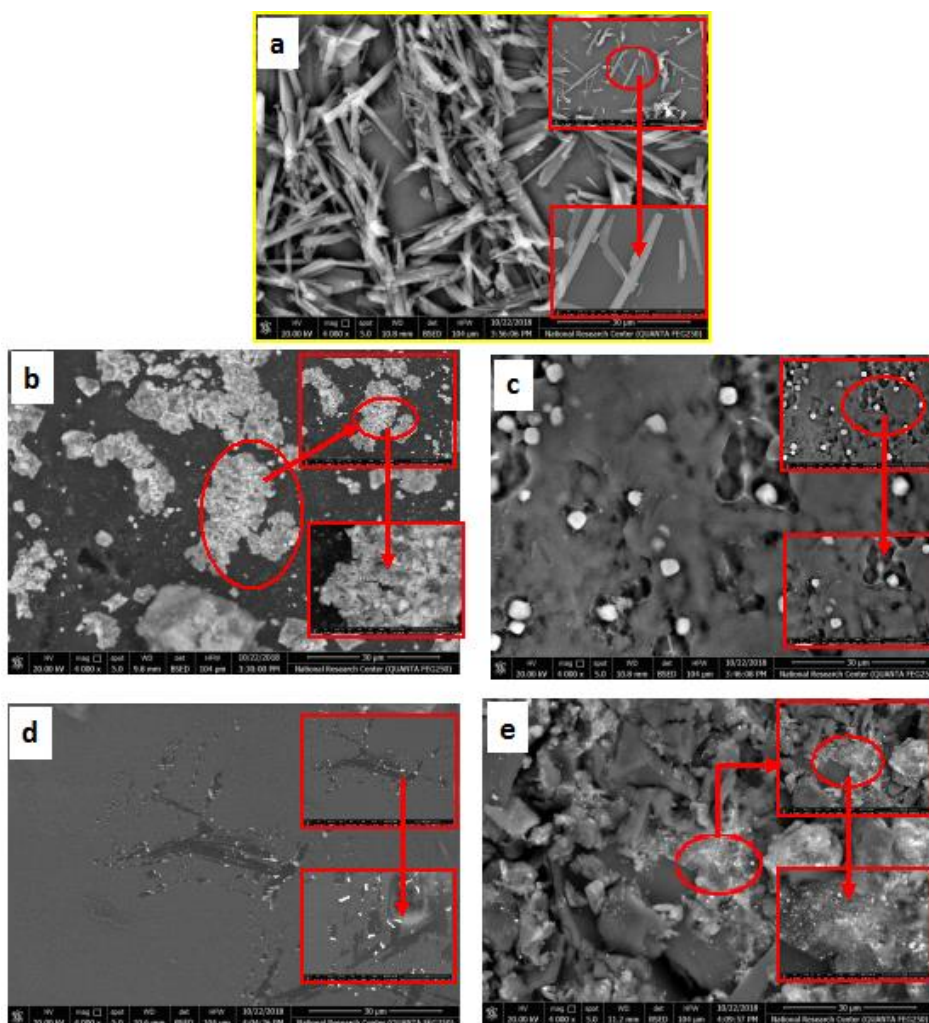


Fig. 2: SEM micrographs of (a) PPCSB (b) Cu(II)PPCSB, (c) Pd(II)PPCSB, (d) AgNPs@PPCSB NBC, (e) AgNPs@Pd(II)PPCSB NBC.

3.3. Antibacterial activities of the as-synthesized compounds

The antibacterial activity (ABA) of new ligand (PPCSB), its M(II)PPCSB complexes (M = Cu, Pd), NBC1 (AgNPs@PPCSB) and NBC2(AgNPs@Pd(II)PPCSB) was investigated against gram positive (*S. aureus*, *B. subtilis*) and gram negative (*E. coli*, *P. aeruginosa*) bacteria using agar plate process.

The images for the antibacterial measurements for the tested compounds are depicted in **Fig. 3** and the calculated zones for the bacterial inhibition (ZOI) are set out in the enclosed table. At first glance, it was found that all tested compounds showed broad-spectrum of ABA. Interestingly, the antibacterial efficacy of PPCSB against *E. coli* is remarkably enhanced upon complexation to M(II) ions and capping of AgNPs (ZOI raised from 0 in case of PPCSB mm to 16 mm for Pd(II)PPCSB). Thus, the metal centre (either ions or NPs) plays a pivotal role in the antibacterial action of new compounds against *E. coli* cells. Unexpectedly, the M(II)PPCSB complexes were found to be more active against all tested bacterial strains than NBCs (AgNPs@PPCSB, AgNPs@Pd(II)PPCSB). Meanwhile, as revealed from ZOI values, the Cu(II)PPCSB is the most potent bactericidal agent against all tested bacterial strains except *E. coli* species which is more affected by Pd(II)PPCSB. On the other hand, the diameter of the inhibition zone is marginally decreased when the Pd(II)PPCSB blended with the *ex-situ* synthesized AgNPs.

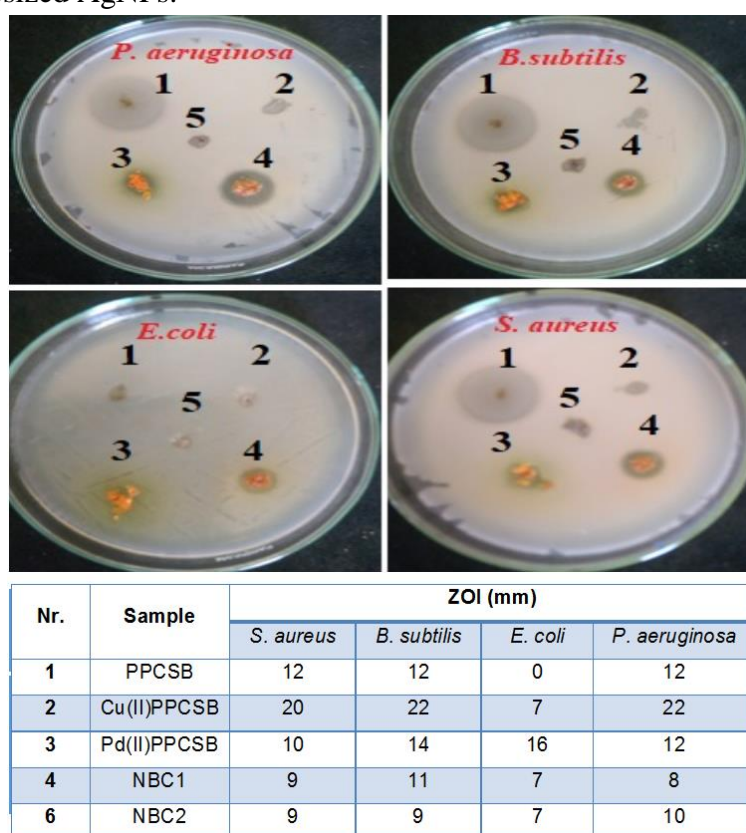


Fig.3: Graph of zone of inhibition (ZOI, mm) for assaying compounds against different microbial species

4- Conclusion

From our work, new chitosan Schiff bases and its Cu (II), Pd (II) complexes and Ag nanocomposites synthesized are eco-friendly materials. The results have shown that these new compounds can be applied as antimicrobial agents in several fields such as pharmaceutical field.

References

- Abdelwahab, H.; Hassan, S.; Yacout, G.; Mostafa, M.; El Sadek, M. Synthesis and biological evaluation of new imine- and amino-chitosan derivatives. *Polymers* 2015, 7, 2690–2700.
- Antony, R.; Theodore David Manickam, S.; Saravanan, K.; Karuppasamy, K.; Balakumar, S. Synthesis, spectroscopic and catalytic studies of Cu(II), Co(II) and Ni(II) complexes immobilized on Schiff base modified chitosan. *J. Mol. Struct.* 2013, 1050, 53–60.
- Baran, T. A new chitosan Schiff base supported Pd(II) complex for microwave-assisted synthesis of biaryls compounds. *J. Mol. Struct.* 2017, 1141, 535–541.
- Choi, B.-K.; Kim, K.-Y.; Yoo, Y.-J.; Oh, S.-J.; Choi, J.-H.; Kim, C.-Y. In vitro antimicrobial activity of a chitoooligosaccharide mixture against actinobacillusactinomycetemcomitans and streptococcus mutans. *Int. J. Antimicrob. Agents* 2001, 18, 553–557.
- Chung, M.J.; Park, J.K.; Park, Y.I. Anti-inflammatory effects of low-molecular weight chitosan oligosaccharides in ige–antigen complex-stimulated RBL-2H3 cells and asthma model mice. *Int. Immunopharmacol.* 2012, 12, 453–459.
- Crini, G. Non-conventional low-cost adsorbents for dye removal: A review. *Bioresour. Technol.* 2006, 97, 1061–1085.
- R.F.M. Elshaarawy, G.A. Seif, M.E. El-Naggar, T.B. Mostafa, E.A. El-Sawi, “*In-situ* and *ex-situ* production of poly-(imidazolium vanillyl)-grafted chitosan/silver nano-biocomposites for eco-friendly antibacterial finishing of cotton fabrics” *Eur. Polymer J.* 2019, 116, 210-221.
- Elshaarawy, R.F.M.; Refaee, A.A.; El-Sawi, E.A. Pharmacological performance of novel poly-(ionic liquid)-grafted chitosan-N-salicylideneschiff bases and their complexes. *Carbohyd.Polym.* 2016, 146, 376–387.
- Elshaarawy, R.F.M.; Janiak, C. Toward new classes of potent antibiotics: Synthesis and antimicrobial activity of novel metallosaldach–imidazolium salts, *Eur. J. Med. Chem.*, 2014, 75, 31-42
- Foster, L.J.R.; Ho, S.; Hook, J.; Basuki, M.; Marçal, H. Chitosan as a biomaterial: Influence of degree of deacetylation on its physiochemical, material and biological properties. *PLoS ONE* 2015, 10, 153-135.
- Garoufis, A.; Hadjikakou, S.K.; Hadjiliadis, N. Palladium coordination compounds as anti-viral, anti-fungal, anti-microbial and anti-tumor agents. *Coord. Chem. Rev.* 2009, 253, 1384–1397.
- Han, T.Y.; Guan, T.S.; Iqbal, M.A.; Haque, R.A.; SharmilaRajeswari, K.; KhadeerAhamed, M.B.; Abdul Majid, A.M.S. Synthesis of water soluble copper(II) complexes: Crystal structures, DNA binding, oxidative DNA cleavage, and in vitro anticancer studies. *Med. Chem. Res.* 2014, 23, 2347–2359.

- Khor, E.; Lim, L.Y. Implantable applications of chitin and chitosan. *Biomaterials* 2003, 24, 2339–2349.
- Miretzky, P.; Cirelli, A.F. Hg(II) removal from water by chitosan and chitosan derivatives: A review. *J. Hazard. Mater.* 2009, 167, 10–23.
- Raman, N.; Selvan, A.; Sudharsan, S. Metallation of ethylenediamine based schiff base with biologically active Cu(II), Ni(II) and Zn(II) ions: Synthesis, spectroscopic characterization, electrochemical behaviour, DNA binding, photonuclease activity and in vitro antimicrobial efficacy. *Spectrochim.ActaA* 2011, 79, 873–883.
- Rinaudo, M. Chitin and chitosan: Properties and applications. *Prog.Polym. Sci.* 2006, 31, 603–632.
- Salama, H.E.; Saad, G.R.; Sabaa, M.W. Synthesis, characterization and biological activity of schiff bases based on chitosan and arylpyrazole moiety. *Int. J. Biol. Macromol.* 2015, 79, 996–1003.
- Verlee, A.; Mincke, S.; Stevens, C.V. Recent developments in antibacterial and antifungal chitosan and its derivatives. *Carbohydr.Polym.* 2017, 164, 268–283.
- Wang, H.; Malhotra, S. V.; Francis, A. J. Toxicity of Various Anions Associated with Methoxyethyl Methyl Imidazolium-Based Ionic Liquids on *Clostridium* sp. *Chemosphere.* 2011, 82, 1597–1603.
- Xia, W.; Liu, P.; Zhang, J.; Chen, J. Biological activities of chitosan and chitooligosaccharides. *FoodHydrocoll.* 2011, 25, 170–179.

الملخص باللغة العربية

تحضير متراكبات البولي فوسفونيم الساليسيل المطعم بقواعد شيف للكتيوزان و دراسة التصميمات فوق الجزيئية للمواد الدوائية متعددة الوظائف يهدف البحث الي تحضير متراكبات البولي فوسفونيم الساليسيل المطعم بمركبات شيف للكتيوزان وتفاعل هذه المركبات مع بعض المعادن مثل نترات الفضة ،اسيتات النحاس وكلوريد الباليوم باستخدام العامل المختزل (صوديوم بوروهيدريد) وتكوين مركبات نانوية جديدة .وقد تم دراسة التقنيات المختلفة للتأكد من هذه المتراكبات مثل الشعبة تحت الحمراء ، وتحليل العناصر ،الرنين النووي المغناطيسي للهيدروجين ،الرنين النووي المغناطيسي للكربون ،حيود الشعبة السينية ،واستخدام الميكروسكوب الإلكتروني الماسح . وقد تم تأثير هذه المتراكبات الجديدة علي انواع مختلفة من البكتيريا موجبة الجرام و بكتيريا سالبة الجرام و وجد ان هذه المتراكبات لها تأثير اكث رعلي بكتيريا سالبة الجرام عن بكتيريا موجبة الجرام.